Environmental Pollution 286 (2021) 117239

Contents lists available at ScienceDirect

Environmental Pollution

journal homepage: www.elsevier.com/locate/envpol

Improving pollutants environmental risk assessment using a multi model toxicity determination with *in vitro*, bacterial, animal and plant model systems: The case of the herbicide alachlor☆,☆☆

Susana P. Pereira [a, b, 1, 2, *], Sandra M.A. Santos [b, 1], Maria A.S. Fernandes [c, 1], Cláudia M. Deus [b], João D. Martins [a, b], Maria C. Pedroso de Lima [b], Joaquim A.F. Vicente [c], Romeu A. Videira [d], Amália S. Jurado [a, b]

[a] Department of Life Sciences, University of Coimbra, 3000-456 Coimbra, Portugal
[b] CNC - Center for Neuroscience and Cell Biology, CIBB - Centre for Innovative Biomedicine and Biotechnology, University of Coimbra, IIIUC - Institute for Interdisciplinary Research, Coimbra, Portugal
[c] IMAR-CMA, University of Coimbra, 3004-517, Coimbra, Portugal
[d] REQUIMTE/LAQV, Laboratory of Pharmacognosy, Department of Chemistry, Faculty of Pharmacy, University of Porto, 4050-313, Porto, Portugal

ARTICLE INFO

Article history:
Received 13 January 2021
Received in revised form
20 April 2021
Accepted 22 April 2021
Available online 27 April 2021

Keywords:
Pollutants
In vitro toxicology
Plant and mitochondria toxicology
Herbicide
Mammalian cell viability

ABSTRACT

Several environmental pollutants, including pesticides, herbicides and persistent organic pollutants play an important role in the development of chronic diseases. However, most studies have examined environmental pollutants toxicity in target organisms or using a specific toxicological test, losing the real effect throughout the ecosystem. In this sense an integrative environmental risk of pollutants assessment, using different model organisms is necessary to predict the real impact in the ecosystem and implications for target and non-target organisms.

The objective of this study was to use alachlor, a chloroacetanilide herbicide responsible for chronic toxicity, to understand its impact in target and non-target organisms and at different levels of biological organization by using several model organisms, including membranes of dipalmitoylphosphatidylcholine (DPPC), rat liver mitochondria, bacterial (*Bacillus stearothermophilus*), plant (*Lemna gibba*) and mammalian cell lines (HeLa and neuro2a).

Our results demonstrated that alachlor strongly interacted with membranes of DPPC and interfered with mitochondrial bioenergetics by reducing the respiratory control ratio and the transmembrane potential. Moreover, alachlor also decreased the growth of *B. stearothermophilus* and its respiratory activity, as well as decreased the viability of both mammalian cell lines. The values of TC_{50} increased in the following order: *Lemna gibba* < neuro2a < HeLa cells < *Bacillus stearothermophilus*. Together, the results suggest that biological membranes constitute a putative target for the toxic action of this lipophilic herbicide and point out the risks of its dissemination on environment, compromising ecosystem equilibrium and human health.

☆ This paper has been recommended for acceptance by Wen Chen.

☆☆ The main findings of this work was that alachlor-induced toxicity in different experimental models emphasized their suitability for toxicity screening and stressed the usefulness of this approach to assess overall environmental risk and prevent eco-toxicological risks impacting human health.

* Corresponding author. CNC – Center for Neuroscience and cell Biology, University of Coimbra UC Biotech Building (Lot 8A) Biocant Park, 3060-197, Cantanhede, Portugal.
E-mail addresses: pereirasusan@gmail.com (S.P. Pereira), marinasantos02@sapo.pt (S.M.A. Santos), mfer@ci.uc.pt (M.A.S. Fernandes), cmcdeus@gmail.com (C.M. Deus), jdgmartins@gmail.com (J.D. Martins), mdelima@ci.uc.pt (M.C. Pedroso de Lima), jvicente@bot.uc.pt (J.A.F. Vicente), rvideira@utad.pt (R.A. Videira), asjurado@bioq.uc.pt (A.S. Jurado).
[1] These authors contributed equally to this work.
[2] New address: Laboratory of Metabolism and Exercise (LaMetEx), Research Centre in Physical Activity, Health and Leisure (CIAFEL), Laboratory for Integrative and Translational Research in Population Health (ITR), Faculty of Sport, University of Porto, 4200-450, Porto, Portugal.

https://doi.org/10.1016/j.envpol.2021.117239
0269-7491/

1. Introduction

During the last decades the use of herbicides has increased dramatically due to intensive agriculture and modifications in farming practices (Piel et al., 2021). Herbicides account for approximately 65% of all pesticide use globally and may have impacts on non-target organisms and their environments (Lerro et al., 2018).

Herbicides mainly enter the environment through application to farm fields or when improperly stored or mixed before application. Herbicides may enter freshwater ecosystems by spray drift, leaching, run-off, or accidental spills. Groundwater contamination may occur when herbicides move from an application or spill on soil into a shallow aquifer presenting potential risks for several aquatic organisms (Mhadhbi and Beiras, 2016). Human unconscious exposure can occur by drinking contaminated water or through skin while bathing in contaminated water (Harper et al., 2020).

Moreover, application of herbicides in soil may result in their adsorption enhancing the accumulation of herbicide concentrations in the topsoil and may endanger crops in the next growing season, or generate weed resistant genotypes that complicates the weed control process and makes control more costly. Moreover, increasing herbicide concentration in the topsoil may damage or change the community structure of the bacterial mats in the soil (El-Nahhal and Hamdona, 2015).

The application of herbicides creates soil and water contamination, resulting in contamination of food samples and agricultural commodities, these contaminations may result in health risks and ecotoxicity with deleterious environmental and public health effects (Dovidauskas et al., 2020; Harper et al., 2020).

Alachlor, 2-chloro-N-[2,6-diethyphenyl]-N-[methoxymethyl] acetamide, a chloroacetanilide herbicide is extensively used for control of annual grasses and many broadleaf weeds in fields of corn, soybeans, and peanuts. Its heavy use and its elevated persistence in water (half-life in ground water is estimated from 808 to 1518 days) amplify the risks for human exposure (Badriyha et al., 2003; Ryberg and Gilliom, 2015). Among the risks of human exposure, diminished sperm quality (affecting sperm concentration and morphology (Grizard et al., 2007)), and the increased incidence of cancer, such as colorectal cancer and leukemia (Lee, 2004) or laryngeal cancer and myeloid leukemia (Lerro et al., 2018). In animals models, namely Wistar rats, alachlor induced nasal (Burman et al., 2003), thyroid and stomach cancers (Acquavella et al., 2004), as well as chromosomal aberrations in bone marrow (Amer et al., 2007). Alachlor is an *in vitro* clastogen (mutagen agent) in human blood lymphocytes (Ladeira and Smajdova, 2017) and in Chinese hamster ovary cells (Lin et al., 1987). Alachlor is also suspected to have endocrine disrupting effects due to the interaction with estrogen and progesterone receptors (Mnif et al., 2011).

Alachlor was present in groundwaters in the USA at levels ranging from less than 0.1–16.6 μg/L (WHO, 2017) exceeding the U.S. Environmental Protection Agency drinking-water maximum contaminant level (MCL) criteria of 2 μg/L for alachlor (Barbash et al., 2001). Despite alachlor being banned as an herbicide in the European Union in 2007 some reports show that even decades after legislative controls, concentrations of pollutants may still pose a risk (Kean et al., 2021).

Biological membranes are an ubiquitous component of cells and their critical role in cell function and viability is recognized from bacteria to superior organisms (Sadura et al., 2020; Zamprogno et al., 2021). Perturbation of membrane biophysical properties leading to severe impairment of cell function has been pointed out as the underlying mechanism for toxicity and disease in a variety of organisms, including humans (Maxfield and Tabas, 2005; Tekpli et al., 2013). The hydrophobicity of alachlor, reflected by a high n-octanol/water partition coefficient (Log K_{OW} = 3.66 (Osano et al., 2002)), makes it prone to exert a membrane-mediated toxic action (Badriyha et al., 2003). In fact, some findings suggest that chloroacetanilides are able to deregulate lipid biosynthesis and unsettle membrane permeability in higher plants (Eckermann, 2003), and it has been reported that alachlor interacts with the components of the plasma membrane (protein and lipids) altering its organization and functions (Fernández et al., 2006). Interference of alachlor with cellular macromolecules such as proteins as also reported by Rattanawong and collaborators, describing that alachlor caused cellular protein degradation of superoxide dismutases and glutathione leading to endogenous oxidative stress (Yi et al., 2007; Rattanawong et al., 2015). It was recently demonstrated in *Saccharomyces cerevisiae* that alachlor-response to oxidative stress requires the iron regulon transcription factor Aft1p, showing a possible correlation between alachlor-induced toxicity and perturbations in metal and antioxidant homeostasis (Gil et al., 2017).

The majority of studies have examined environmental pollutants toxicity in target organisms using a specific toxicological test, losing the real effect throughout the ecosystem. In this sense an integrative environmental risk of pollutants assessment, using different model organisms, are necessary to predict the real impact in the ecosystem and implications for target and non-target organism. The main objective of the present study was performing a toxicological screening of alachlor using several model organisms and understand its impact at different levels of biological organization, from subcellular through to organism level, as a methodology to improve pollutants environmental risk assessment using a comparative multi model toxicity determination. With this purpose, several *in vitro* model systems were used in the present study: synthetic membranes of dipalmitoylphosphatidylcholine (DPPC), rat liver mitochondria, bacterial (*Bacillus stearothermophilus*) and mammalian cells (HeLa and neuro2a), and a plant organism (*Lemna gibba*), which was used as a positive control. These models were chosen because they are known to be suitable tools for toxicity assessment of a variety of environmental pollutants (Pereira et al., 2009; Machado et al., 2010; Perreault et al., 2010; Chowdhary et al., 2020; Yuan et al., 2020). The concentrations of herbicide that cause 50% inhibition of bacterial or plant growth and 50% loss of mammalian cell viability (TC_{50}), relative to the respective untreated controls, were calculated in order to compare alachlor toxicity in a model of a target organism (the plant *Lemna gibba*) with two models of "non-target" organisms (bacteria and mammalian).

This work highlights not only the use of different model systems representing both target and non-target organisms to evaluate the eco-toxicological risks of the dissemination of lipophilic herbicides on environment but also forewarning the need for a broader assessment of pollutants impact to prevent compromising ecosystem equilibrium and human health.

2. Materials and methods

2.1. Chemicals

All chemicals, including the synthetic lipid dipalmitoylphosphatidylcholine (DPPC, 99%) and the fluidity probe 1,6-diphenyl-1,3,5-hexatriene (DPH), were obtained from Sigma Chemical Company (St Louis, MO, USA). Alachlor (2-chloro-N-[2,6-diethyphenyl]-N-[methoxymethyl] acetamide) with 99.5% purity was dissolved in dimethyl sulfoxide (DMSO, 99.5%) and saved in hermetically closed glass tubes at −20 °C for minimizing evaporation. Reagents of high purity (≥95%) were used in all experimental procedures.

2.2. Preparation of multilamellar vesicles (MLV) of DPPC

The multilamellar vesicles of DPPC were prepared in accordance with a protocol previously described (Fernandes et al., 2008). Aliquots of pure DPPC in chloroform were dispersed in round bottom flasks and the solvent was evaporated until a dry lipid film was formed and it was hydrated under N_2 atmosphere with an appropriate volume of a solution containing 50 mM KCl and 10 mM Hepes, pH 7.4, by hand shaking at 50 °C, to obtain a lipid concentration of 150 mM and 350 μM for differential scanning calorimetry (DSC) and fluorescence polarization measurements, respectively. Then, the suspension was stirred under vortexing and stabilized overnight.

2.3. Differential scanning calorimetry (DSC) measurements

An aliquot of concentrated alachlor was added to 150 mM DPPC aqueous dispersions, to yield herbicide/lipid molar ratios of 1/10 and 1/5. Lipid dispersions were allowed to equilibrate for 18–20 h at 50 °C, and subsequently hermetically sealed in aluminum pans, and thermograms were then recorded in a PerkinElmer Pyris 1 DSC. The DSC measurements were performed as described (Fernandes et al., 2008). Data acquisition and analysis were performed using the software provided by PerkinElmer. Due to the supercooling phenomenon, accurate thermotropic transitions were evaluated from heating traces. The onset and completion of the phase transition (T_o and T_f) were determined from the intersections of the peak slopes with the baseline of the thermograms (Koynova et al., 1985), allowing the determination of the transition temperature range (T_f-T_o), and T_m corresponds to the temperature at the peak. At the end of the experiments, the aluminum pans were opened, and the samples dissolved in a chloroform/methanol (5/1) mixture. The phospholipid content was determined by measuring inorganic phosphate (Bartlett, 1959) after hydrolysis of the extracts at 180 °C in 70% $HClO_4$ (Böttcher et al., 1961).

2.4. Fluorescence polarization measurements

The fluidity probe 1,6-diphenyl-1,3,5-hexatriene (DPH) in dimethylformamide was injected into the liposome suspension (350 μM), prepared according to the procedure previously described in section 2.2, to give a lipid/probe molar ratio of 200. The mixture was vortexed for 10 s, and then alachlor was added to yield the herbicide/lipid molar ratios of 1/10 and 1/5. The mixtures were incubated at 50 °C in the dark, for a period of 18–20 h, to reach equilibrium. A control sample was prepared without alachlor, but with a DMSO volume equivalent to the maximal volume of herbicide used. This solvent volume had insignificant effects (Dludla et al., 2018) on the fluorimetric measurements. This assay was performed in a PerkinElmer spectrofluorimeter (model MPF-3) equipped with a thermostatic cell holder. The excitation and emission wavelengths were set at 336 nm and 450 nm, respectively (5 nm excitation and 6 nm emission band pass). All fluorescence measurements were corrected for the contribution of light scattering by using appropriate blanks (without probe, but with an equivalent volume of dimethylformamide).

The probe was excited with vertically polarized light and resulting fluorescence intensity was recorded with the emission polarizer oriented parallel (I_{II}) and perpendicular ($I \perp$) to the excitation polarizer allowing the determination of steady-state fluorescence polarization by the following equation (Shinitzky and Barenholz, 1978): $P = (I_{II} - G\ I \perp)/(I_{II} + G\ I \perp)$, where G is the grating correction factor given by the ratio of vertically to horizontally polarized emission components, when the excitation light is polarized in the horizontal direction. In the fluorescence polarization thermogram three critical temperature values were defined: T_o and T_f, spotting the extreme temperatures where abrupt changes of the fluorescence polarization occur, and T_m reflecting the midpoint of the main transition and corresponding to the peak of the fluorescence polarization first derivative curve. Transition temperatures were obtained as the mean value of three independent experiences.

2.5. Animals and isolation of rat liver mitochondria

Male Wistar rats (250–350 g), housed at 22 ± 2 °C under artificial light for 12 h light/dark cycle and with access to water and food *ad libitum*, were used throughout the experiments, which were carried out in accordance with the National Requirements for Vertebrate Animal Research and the European Convention for the Protection of Animals used for Experimental and other Scientific Purposes. Mitochondria were isolated from the liver of male Wistar rats by differential centrifugation, according to conventional methods (Pereira et al., 2009). After washing, the pellet was gently resuspended in the washing medium (250 mM sucrose and 10 mM HEPES-KOH, pH 7.2) at a protein concentration of about 50 $mg.ml^{-1}$. Protein content was determined by the biuret method (Gornall et al., 1949).

2.6. Bacterial cultures and isolation of protoplasts

The strain of *B. stearothermophilus* was supplied by Mast Laboratories, UK. The maintenance and growth conditions have been previously described. Alachlor was added to the growth medium from a concentrated solution in order to obtain a final concentration ranging from 300 to 500 μM. Growth was monitored by measuring the turbidity (optical density, OD) at 610 nm, in a Bausch and Lomb Spectronic 21 spectrophotometer.

Protoplasts were obtained essentially as described by Wisdom and Welker (1973). The protein content of the protoplasts was determined by the biuret method, using a calibration curve with bovine serum albumin (Gornall et al., 1949).

2.7. Measurement of bacterial and mitochondrial respiration

The respiratory activity of bacterial protoplasts was monitored polarographically with a Clark oxygen electrode in accordance with the protocol previously described (Pereira et al., 2009). Aliquots of a concentrated alachlor solution were added to the reaction medium containing the protoplasts, and each preparation was incubated for 30 min, before the addition of the respiratory substrate. Oxygen consumption rate in the presence of the herbicide was expressed as % of the control.

Mitochondria oxygen consumption was monitored with a Clark-type electrode as previously described (Pereira et al., 2009). Mitochondria were incubated for 3 min with different alachlor concentrations, before energization with 10 mM malate/5 mM glutamate or 10 mM succinato in the presence of 2 μM rotenone. To induce state 3 respiration, adenosine diphosphate (ADP, 200 μM) was added. Uncoupled respiration was initiated by the addition of 1 μM p-trifluoromethoxyphenylhydrazone (FCCP). O_2 consumption was calculated considering that the saturation oxygen concentration was 232 nmol O_2 per ml of reaction medium at 30 °C. Control values are expressed in nmol $O_2.mg^{-1}$ protein.min^{-1}. The respiratory control ratio (RCR) and ADP to oxygen ratio (ADP/O) were calculated according with previously described methods (Chance and Williams, 1956).

2.8. Cell culture and evaluation of cell viability

HeLa cells (human epithelial cervical carcinoma cell line) and neuro2a cells (mouse neuroblastoma cell line), maintained at 37 °C under 5% CO_2, in Dulbecco's modified Eagle's medium−high glucose (DMEM−HG; Sigma, St. Louis, MO), supplemented with 10% (v/v) heat inactivated fetal bovine serum (FBS; Sigma, St. Louis, MO), penicillin (100 U/ml) and streptomycin (100 μg/ml), were grown in monolayer and detached by treatment with 0.25% trypsin solution (Sigma, St. Louis, MO). HeLa and neuro2a cells were seeded at a density of 4.5×10^4 cells/ml of medium onto 48-well culture plates. After 24 h, cells reached 50−70% confluence and were incubated with alachlor solution at different concentrations (10 μM−1000 μM) or with DMSO at a volume equivalent to the maximal volume of herbicide solution used in the assay (control), at 37 °C for 24 h.

The cytotoxicity induced by the herbicide in HeLa and neuro2a cells was evaluated by a modified Alamar Blue colorimetric assay, as previously described (Cardoso et al., 2011). The absorbance was measured in a SPECTRAmax PLUS 384 spectrophotometer (Molecular Devices, Union City, CA) at 570 (A_{570}) and 600 nm (A_{600}) (supplier indication). The percentage of cytotoxicity for each herbicide concentration was calculated according to the equation: % cytotoxicity = $100 - [((A_{570} - A_{600})_{\text{of treated cells}})/((A_{570} - A_{600})_{\text{of control cells}})] \times 100$.

The TC_{50} values (alachlor toxic concentration at which cell viability reaches 50% of that of the control culture) were determined from the plots of cytotoxicity data against herbicide concentrations by interpolation.

2.9. Lemna gibba growth and chlorophyll extraction/quantification

Lemna gibba plants, collected from an artificial pond in the Portuguese Vila Real de Trás-os-Montes e Alto Douro University campus, were cultured as previously described (Santos et al., 2013).

Alachlor solution was added in order to obtain concentrations ranging from 2.5 to 100 μM. A control sample was prepared without alachlor, but with a DMSO volume equivalent to the maximal volume of herbicide used. Plants were incubated during 7 days in a culture growth chamber at 20 ± 2 °C under a photosynthetically active radiation (50 μmol/m^2/s; Conviron mod. E7/2). Alachlor effects were assessed considering the frond number and the fresh weight, according to the standard guideline 221 (OECD, 2002). The relative growth rate (RGR) was calculated according to equation: $RGR = (\ln x_2 - \ln x_1)/(t_2 - t_1)$, where x_1 and x_2 are the frond numbers at time t_1 (0 days) and t_2 (7 days), respectively (Kufel et al., 2012). Data are expressed as percentage of those obtained with a control culture (grown in the absence of alachlor). The evaluation of chlorophyll content present in the *Lemna gibba* treated with alachlor was performed in accordance with (Santos et al., 2013). The concentrations of chlorophyll *a* (Chl a), chlorophyll *b* (Chl b) and total chlorophyll were calculated by the following equation (Lichtenthaler and Wellburn, 1983): Chl a (μg/mL) = $12.21A_{663} - 2.81A_{646}$; Chl b (μg/mL) = $20.13A_{646} - 5.03A_{663}$; total chlorophyll = Chl a + Chl b. All values were normalized with respect to plant fresh weight.

2.10. Statistical analysis

All data were obtained from three or more independent experiments, using different preparations. The values are expressed as mean ± standard deviation (SD) or mean ± standard error of the mean (SEM). Means were compared using one-way analysis of variance (ANOVA) with the student-Newman-Keuls as a post hoc test. Differences were considered significant if: *$p < 0.05$; **$p < 0.01$ and ***$p < 0.001$. Statistical analyses were performed using Graph Pad Prism version 5.

3. Results

3.1. Effects of alachlor on membrane physical properties

The interaction of the herbicide alachlor with multilamellar vesicles (MLV) prepared with the synthetic lipid DPPC was studied by fluorescence polarization of DPH and DSC. The DPH probe is preferentially located in the hydrophobic interior of the bilayer, allowing the evaluation of the structural organization of lipids in the central region of the membrane. The effects exerted by alachlor upon interaction with DPPC membranes, at different concentrations, were evaluated in terms of several parameters (listed in Table 1), which reflect the extent of the perturbation promoted by the herbicide in the physical state of DPPC bilayers. The phase transition detected by fluorescence polarization of DPH underwent a broadening and a shift to lower temperatures in the presence of increasing concentrations of alachlor. Thus, the T_m (midpoint temperature of thermotropic phase transition) decreased from 42.2 °C, under control conditions, to 39.6 °C in the presence of alachlor at a molar ratio herbicide to lipid of 1/5, and the transition temperature amplitude increased from 3.2 to 6.1 °C under identical conditions. As illustrated in Table 1, similar results were obtained by DSC for these thermodynamic parameters. The values of ΔH (J/g) for the main transition of DPPC liposomes, in the absence of alachlor and at the 1/10 and 1/5 alachlor/lipid molar ratios are also displayed in Table 1. Fig. 1 shows DSC heating scans of DPPC MLV incorporating increasing concentrations of alachlor, in the range of 0.1 (1/10) to 0.2 (1/5) alachlor/DPPC molar ratio. In the absence of herbicide, DPPC dispersions exhibited a sharp endotherm, centered at 43.7 °C, with a ΔH value of 60.4 J/g (Table 1). Increasing concentrations of alachlor significantly affected all characteristic parameters of DPPC endotherms, promoting a broadening of the endotherm and its shift to lower temperatures. At the molar ratio alachlor/DPPC of 1/5, the endotherm, centered at 39.1 °C, showed a ΔH value of 51.78 J/g and the amplitude of the transition temperature range revealed a significant increase as compared to the control preparation (from 3.4 °C in the control to 7.8 °C at 1/5 alachlor/DPPC molar ratio). At the highest alachlor concentration, the endotherm showed a clear asymmetry, denoting the occurrence of a lateral phase separation.

3.2. Effects of alachlor on mitochondrial bioenergetics

The effects of alachlor on glutamate/malate- and succinate-supported state 4 and state 3 respiration rates and respiratory indices RCR and ADP/O ratio of rat liver mitochondria are depicted in Fig. 2.

State 4 respiration was not significantly stimulated whereas state 3 respiration was inhibited by alachlor concentrations up to 1.2 μmol/mg protein (approximately 60% with alachlor at 1 μmol/mg protein), either using glutamate/malate or succinate as the respiratory substrates (Fig. 2A and C). The FCCP-uncoupled respiration was inhibited by alachlor at the same extent at which state 3 respiration was depressed (data not shown). In the same concentration range, alachlor significantly depressed RCR (from about 6 to less than 2) with both respiratory substrates. The ADP/O ratio was also decreased from 2.86 to 2.16 with glutamate/malate and from about 1.88 to 1.28 with succinate (Fig. 2). Alachlor induced $\Delta\psi$ dissipation and a depression of the phosphorylation rate when glutamate/malate or succinate were used to energize mitochondria (Fig. 3A). Thus, in the presence of alachlor at 0.8 μmol/mg protein, succinate-dependent $\Delta\Psi$ underwent a dissipation of 15% (Table 2)

Table 1
Effects of alachlor on the thermotropic behavior of DPPC dispersions, as assessed by Fluorescence Polarization of DPH and Differential Scanning Calorimetry. T_0, T_m, $T_f - T_0$, and ΔH correspond, respectively, to the onset, midpoint, amplitude and enthalpy change for the main transition of DPPC liposomes.

	Alachlor/DPPC (molar ratio)	Fluorescence Polarization[a]	Differential Scanning Calorimetry[a,a]
T_0 (°C)	control	41.30 ± 1.47	42.52 ± 0.43
	1/10	38.02 ± 0.97 *	38.14 ± 0.79 ***
	1/5	35.27 ± 1.41 ***	34.83 ± 0.64 ***, °°°
T_m (°C)	control	42.16 ± 0.78	43.66 ± 0.51
	1/10	41.20 ± 0.20[n.s.]	41.40 ± 0.43 **
	1/5	39.62 ± 0.54 *	39.09 ± 0.58 ***, °°
T_f - T_0 (°C)	control	3.20 ± 0.20	3.39 ± 0.11
	1/10	5.60 ± 0.20 ***	6.24 ± 1.72 *
	1/5	6.10 ± 0.25 ***	7.83 ± 1.41 **
ΔH (J/g)	control		60.41 ± 1.26
	1/10		56.33 ± 2.34[n.s.]
	1/5		51.76 ± 1.43 ***

[a] Results are means ± standard deviation from three or more independent experiments and comparisons were performed using one way ANOVA, with the Student–Newman–Keuls as a post hoc test, for the following paired observations: control (0 μM alachlor) *vs.* different concentrations of alachlor (n.s., not significant; *p < 0.05; **p < 0.01; ***p < 0.001); different alachlor concentrations *vs.* the concentration immediately below (n.s., not significant; °°p < 0.01; °°°p < 0.001).

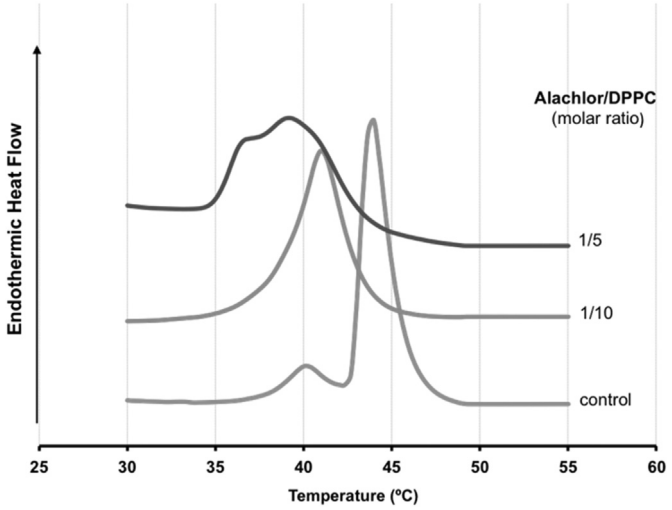

Fig. 1. DSC heating scans of DPPC liposomes in the absence (control) and in the presence of alachlor, at the molar ratios alachlor/DPPC of 1/10 and 1/5.

and the phosphorylation rate was depressed by 74% (Fig. 3A). These effects were significantly stronger than those observed for glutamate/malate: 10% for ΔΨ dissipation (Table 2) and 64% for phosphorylation depression (Fig. 3A). However, when ascorbate/TMPD were used as respiratory substrate, alachlor dissipated Δψ but did not affect the phosphorylation rate at concentrations up to 0.8 μmol/mg protein (Fig. 3B).

3.3. Alachlor effects on bacterial respiration

Protoplasts prepared from cells of *B. stearothermophilus*, grown in the basal medium at 65 °C, were used to assess the effect of alachlor on the respiratory activity of the bacterium. Protoplasts were incubated with alachlor in the concentration range of 1.0–3.0 μmol/mg of protein, during a period of 30 min preceding the supplementation with the respiratory substrate. The NADH-supported oxygen consumption rate, expressed in percentage of the control (protoplasts incubated with a volume of DMSO corresponding to the maximum amount of alachlor solution assayed in the respiration experiment), exhibited a progressive decrease with increasing concentrations of the herbicide, as documented in Table 3. At the concentration of 1 μmol/mg of protein, the herbicide already promoted a significant decrease of the respiratory rate (by 26.6%). When a mixture of ascorbate + TMPD was used instead of NADH as respiratory substrate, alachlor did not exert any significant effect on the respiratory activity of the protoplasts in the concentration range of 1–3 μmol/mg of protein (data not shown). The oxygen consumption supported by NADH or ascorbate + TMPD was completely impaired by the addition of KCN (1 mM), as a consequence of complete inhibition of the terminal oxidase (data not shown).

3.4. Effects of alachlor on bacterial growth

B. stearothermophilus was grown at 65 °C (within the optimal temperature range) in a complex medium (dilute L-Broth) supplemented with alachlor to obtain a final concentration ranging from 100 to 500 μM. As a control, a culture was grown in a medium without herbicide but containing DMSO at a volume corresponding to the maximal amount of alachlor solution assayed in the growth experiment. According to the results shown in Fig. 4, alachlor inhibited bacterial growth as a function of concentration, inducing a progressive increase of the lag time, a decrease of the specific growth rate and a decrease of the final cell density (Table 4).

As observed, at the concentration of 500 μM, alachlor reduced the specific growth rate by approximately 36% and promoted a decay of cell yield of about 42%, as compared to the control culture (Table 4). Although plotting the growth parameters as a function of the herbicide concentration did not allow to accurately determine the TC_{50} values of alachlor, these were inferred to be higher than 500 μM (Table 4).

3.5. Effects of alachlor on mammalian cell viability

The cytotoxicity of alachlor was evaluated in two mammalian cell lines, neuro2a (from rat neuroblastoma) and HeLa cells (from human cervical cancer), using the Alamar Blue assay. The Alamar Blue reagent is a redox indicator corresponding to the oxidized form of the resazurin dye, which changes the color and becomes fluorescent when reduced. Thus, this resazurin-based assay evaluates cell metabolic activity, reflecting the presence of a reducing environment, which is characteristic of viable cells (Silva et al., 2016).

The toxicity exerted by alachlor was determined after 24 h of incubation with the cells at different concentrations of the compound, in the range of 10–1000 μM (Fig. 5). As observed, the herbicide promoted a concentration-dependent cytotoxic effect,

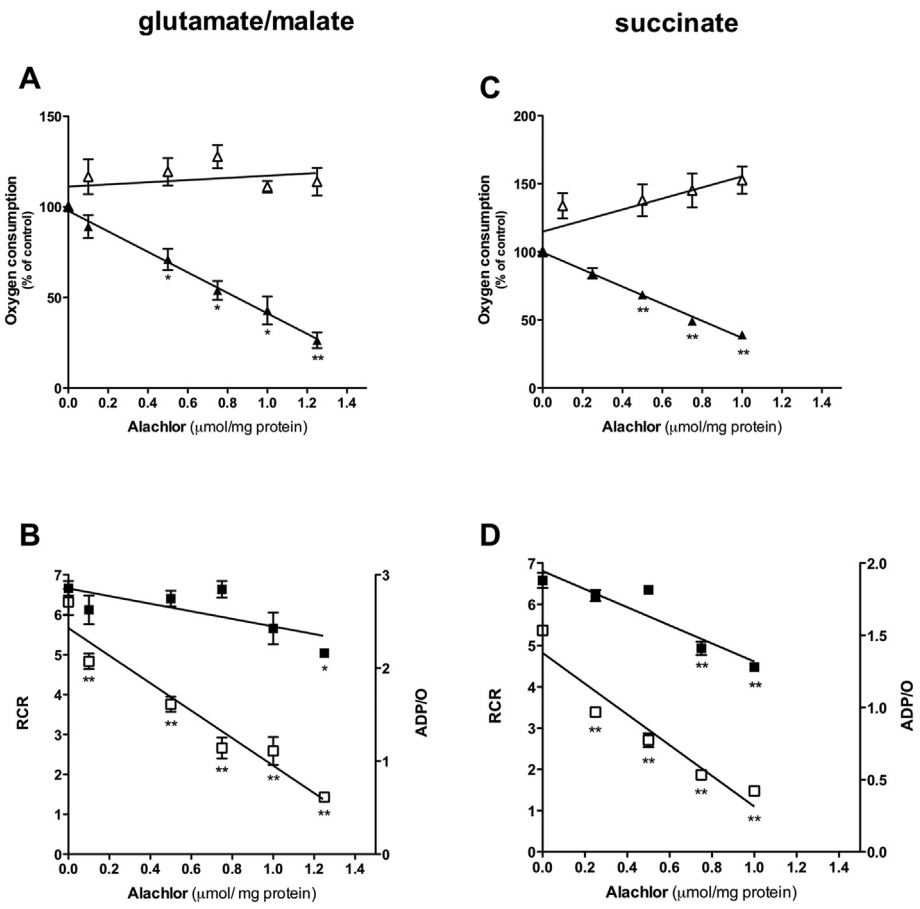

Fig. 2. Effects of alachlor on glutamate/malate- and succinate-supported respiratory activity (complexes I and II, respectively) of rat liver mitochondria. (**A**) Glutamate/malate-supported O_2 consumption rates in state 4 (open triangles) and state 3 (filled triangles) respiration, expressed as percentage of the control. (**B**) Glutamate/malate-supported respiratory indices RCR (opened squares) and ADP/O (closed squares). (**C**) Succinate-supported O_2 consumption rates in state 4 (open triangles) and state 3 (filled triangles) respiration, expressed as percentage of the control. (**D**) Succinate-supported respiratory indices RCR (opened squares) and ADP/O (filled squares). Control values of O_2 consumption rates (corresponding to 100%) in the respiration states 4 and 3 were, respectively, 4.87 ± 0.70 and 30.4 ± 0.94 nmol O_2 .mg^{-1} protein. min^{-1} in A and 6.7 ± 0.67 and 36.0 ± 3.0 nmol O_2.mg^{-1} protein.min^{-1}, in C. The results correspond to the mean ± SEM of three experiments performed with different mitochondrial preparations. Comparisions relative to the control (mitochondria without alachlor) were performed using one-way ANOVA with the Student-Newman-Keuls as post hoc test (*p < 0.05; **p < 0.01).

reflected by a decrease of cell viability with increasing herbicide concentrations. Typical dose-response curves were obtained by plotting the percentage of cytotoxicity with respect to a control without herbicide (containing DMSO at a volume corresponding to the maximal amount of alachlor solution assayed in the viability experiments), corresponding to 100% cell viability or 0% of cell toxicity, against herbicide concentration. From the TC_{50} values (alahlor concentrations at which cell viability reached 50% of that of the control), it became apparent that alachlor exerted a stronger toxicity in neuro2a cells (TC_{50} = 68.9 μM) than in HeLa cells (TC_{50} = 235.5 μM). Although the dose/response curve of alachlor showed a shift to lower herbicide concentrations in neuro2a cells as compared to that in HeLa cells, the curves approached each other at the highest concentrations, which reveals that, at these concentrations, alachlor promoted a loss of viability of about 90% in both cell types.

3.6. Alachlor effects on L. gibba growth and chlorophyll content

The effects of alachlor on the vegetative proliferation of *Lemna gibba* were evaluated in the presence of increasing herbicide concentrations (2.5–100 μM) and compared to a control culture, grown in the absence of alachlor and with a DMSO volume equivalent to the maximal volume of herbicide used. As shown in Fig. 6A, *Lemna gibba* growth rate, determined by counting the frond number at the beginning and at the end of a period of seven days (as described in Material and Methods section) decreased with increasing concentrations of alachlor. In the concentration range of 2.5–10 μM of the herbicide, the growth rate decreased abruptly, but at higher concentrations, up to 100 μM, the decrease was slower. The impact of the herbicide on plant chlorophyll content was also evaluated (Fig. 6B). A decrease in the total content of chlorophylls was noticed with increasing alachlor concentrations, although a significant effect has been detected only at concentrations of 10 μM or higher.

4. Discussion

The herbicidal properties of chloroacetanilides (in which group, alachlor is included (Jurado et al., 2011)) are assumed to be caused by the inhibition of the elongase system responsible for the formation of very long chain fatty acids (VLCFA) in plants, leading to the impairment of structure and function of the plasma membrane (Böger, 2003; Eckermann, 2003; Trenkamp et al., 2004), and the inhibition of cell division (Marc et al., 2002; Hemanth Kumar and Jagannath, 2020) and protein synthesis (El-Hadary and Chung, 2013).

Alachlor effects on non-target organisms have also been reported in the literature (Seok et al., 2012; Rattanawong et al., 2015;

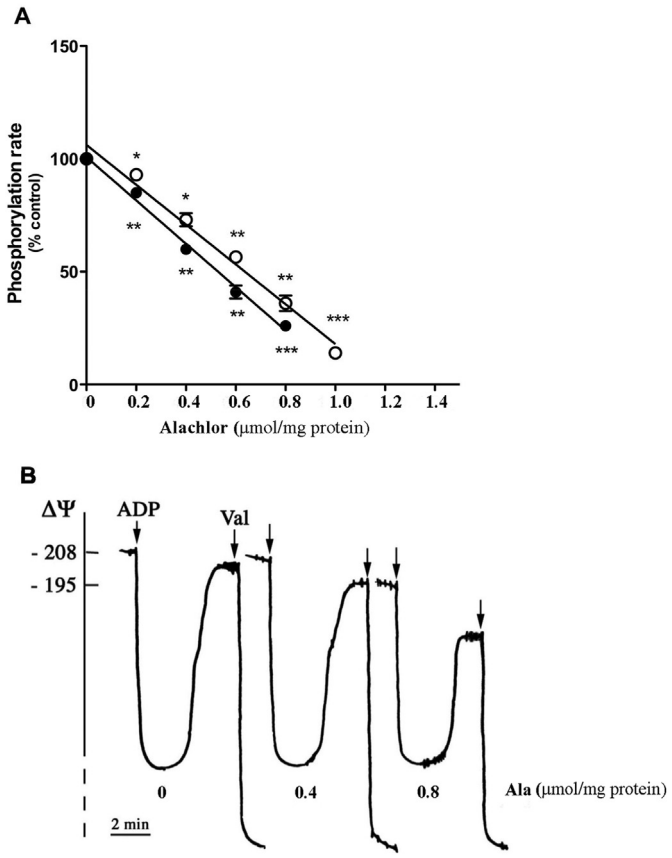

Fig. 3. Effects of alachlor on phosphorylation rates and transmembrane potential (ΔΨ) of rat liver mitochondria. (**A**) Phosphorylation rates with glutamate/malate (open circles) and succinate (filled circles). Control values of phosphorylation rates (corresponding to 100%) with glutamate/malate and succinate as respiratory substrates were, respectively, 148.5 ± 3.18 and 130.5 ± 7.22 nmol ADP. mg^{-1} protein. Min^{-1}. (B) Ascorbate/TMPD-dependent transmembrane potential (ΔΨ); ADP (200 nmoles) initiated the phosphorylation; 1 μM valinomycin was used to dissipate the transmembrane potential. Traces of ΔΨ fluctuations are represented for three preparations: a control preparation (without alachlor) and two preparations containing alachlor (Ala) at the concentrations of 400 and 800 μM. Data in **A** correspond to the mean ± SEM of three experiments performed with different mitochondrial preparations and traces in B are typical of three experiments using different mitochondrial preparations. Comparisions relative to the control (mitochondria without alachlor) were performed using one-way ANOVA with the Student-Newman-Keuls as post hoc test (*p < 0.05; **p < 0.01).

Table 2
Effects of increasing concentrations of alachlor on the transmembrane potential (ΔΨ) of rat liver mitochondria.

Alachlor (μmol/mg protein)	Δψ (mV)[a]	
	Malate/Glutamate	Succinate
0	−217 ± 1.5	−215 ± 0.9
0.2	−215 ± 1.2	−213 ± 0.9
0.4	−210 ± 0.3	−209 ± 0.8
0.6	−207 ± 0.6 *	−199 ± 3,1 *
0.8	−197 ± 1,7 *	−184 ± 2,3 **

[a] Values are means ± standard error from three independent experiments using different mitochondrial preparations. *p < 0.05; **p < 0.01 *vs* control (in the absence of alachlor).

Gil et al., 2017). Following our previous data concerning the capacity of the chloroacetanilide herbicide metolachlor to inhibit bacterial growth and respiratory activity and to impair mitochondrial bioenergetics (Pereira et al., 2009), in the present work we performed a comprehensive study on the toxicity exerted by

Table 3
Effects of alachlor on the oxygen consumption rate of *B. stearothermophilus* protoplasts using NADH as substrate.

Alachlor (μmol/mg protein)	O_2 consumption rate (% of the control)[a]
0.00	100.00
1.00	73.43 ± 1.45 ***
2.00	60.58 ± 6.46 ***, °°
3.00	23.79 ± 2.01 ***, °°°

[a] Results are means ± standard deviation from at least three independent experiments and are expressed as percentage of the control (without alachlor). Comparisons were performed using one way ANOVA, with the Student−Newman−Keuls as a post hoc test, for the following paired observations: protoplasts incubated with alachlor at different concentrations *vs* control protoplasts (***p < 0.001) or protoplasts incubated in the presence of alachlor at different concentrations *vs* protoplasts incubated with alachlor at the concentration immediately below (°°p < 0.01; °°°p < 0.001).

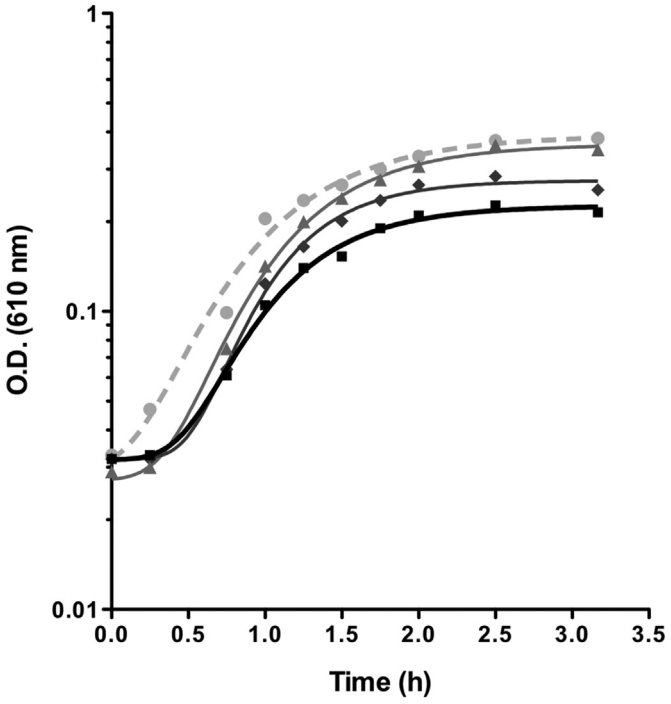

Fig. 4. Effect of alachlor on the growth of cultures of *Bacillus stearothermophilus*, at 65 °C. Cells were incubated in a basal-medium (diluted L-Broth) without additives (control, filled circles) and in the presence of alachlor at 300 μM (filled triangles), 400 μM (filled diamonds) and 500 μM (filled squares) and growth was monitored by optical density (O.D.) measurements. The results shown are representative of three independent experiments using different bacterial preparations.

alachlor, in a broader spectrum of biological systems, since toxic responses can vary substantially depending on the species. Although alachlor is used to kill weeds, once it is released into the ecosystem it can spread and affect other organisms (Sopeña et al., 2009). In this sense, while in the previous studies a Gram-positive bacterium, their protoplasts and rat liver mitochondria were used as a models (Pereira et al., 2009), in the present work other biological models that have been recognized to be useful to chemical toxicity screening assays were used, including mammalian cell cultures and the aquatic plant *Lemna gibba*. As an approach to investigate whether toxicological effects of alachlor would be mediated by perturbation of biomembrane physical properties, biophysical studies with a membrane-mimicking model (DPPC liposomes) were also conducted.

Several studies have demonstrated that mitochondrial function

Table 4
Effects of increasing concentrations of alachlor on growth parameters (specific growth rate and final cell density) of *B. stearothermophilus*. Estimated TC_{50} values of alachlor (at μM) are presented for both growth parameters.

Alachlor (μM)	Specific growth rate (h^{-1})[a]	Final cell density (% of control)[a]
0	2.48 ± 0.16	100
300	2.29 ± 0.17$^{n.s.}$	92.68 ± 4.21$^{n.s.}$
400	1.66 ± 0.05 **$^{\circ}$	80.81 ± 6.07 ***$^{\circ\circ}$
500	1.58 ± 0.31***	57.91 ± 3.91 ***$^{\circ\circ\circ}$
TC_{50} (μM)	>500	>500

[a] Values of specific growth rates and final cell densities are means ± standard deviation from three or more independent experiments and comparisons were performed using one way ANOVA, with the Student−Newman−Keuls as a post hoc test, for the following paired observations: control culture (0 μM alachlor) *vs* cultures grown in the presence of alachlor at different concentrations (n.s., not significant; **p < 0.01; ***p < 0.001); cultures grown in the presence of alachlor at different concentrations *vs* cultures grown in the presence of alachlor at the concentration immediately below (n.s., not significant; °p < 0.05; °°p < 0.01; °°°p < 0.001).

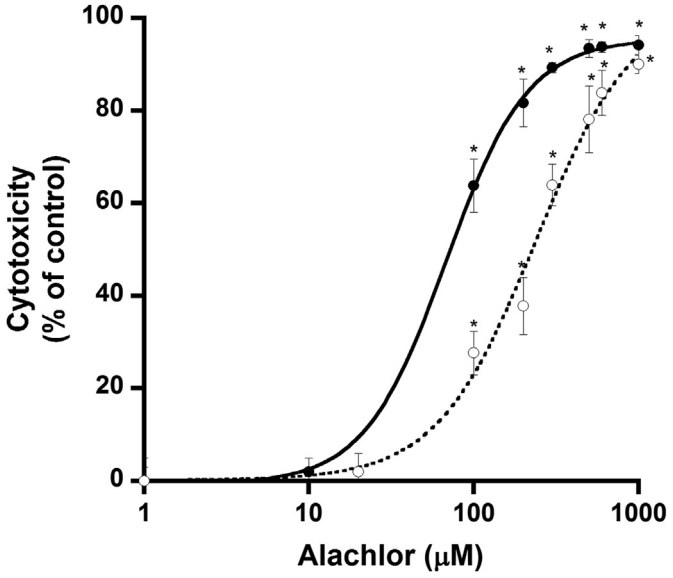

Fig. 5. Cytotoxicity of alachlor in neuro2a cells (closed circles) and HeLa cells (open circles). The cells were incubated with alachlor over the concentration range of 10–1000 μM in Dulbecco's modified Eagle's medium (DMEM-HG) for 24 h. Cell viability was determined by the Alamar blue assay, as described in Materials and Methods. The data are expressed as percentage of a control (untreated cells). Mean ± SD were obtained from triplicates and are representative of three independent experiments. Comparisons relative to the control were performed using one-way ANOVA with the Student-Newman-Keuls as post hoc test (*p < 0.05).

is altered by exposure to different herbicides (Bora et al., 2021; Park et al., 2021). In fact, it was described that atrazine exposure upregulated the expression of proapoptotic factors, namely Bax, Caspase 3 and FasL, and downregulated antiapoptotic factor, such as Bcl-2. Moreover, atrazine-exposed quail kidney have mitochondrial abnormalities and oxidative damage that occurred by atrazine influence in mitochondrial-related genes expression and modulation of NRF2 signaling pathway (Zhang et al., 2018). Moreover Pendimethalin, an herbicide used to control weeds, interfered with mitochondrial complexes I and V inhibiting energy metabolism in zebrafish embryos (Park et al., 2021). Similarly, we showed that alachlor interferes with mitochondrial bioenergetics of rat liver mitochondria. However, the Complex IV was not affected by alachlor, as deduced from ΔΨ records. Thus, although some dissipation of ΔΨ was detected, the phosphorylation rates of ascorbate/TMPD-energized mitochondria were not affected. These results suggested that alachlor intervenes directly at Q binding sites between complex I and III or II and III, as previously described for other herbicides, including atrazine (Lim et al., 2009). The oxygen consumption rate of *B. stearothermophilus* protoplasts show to be unaffected when ascorbate/TMPD was used as a respiratory substrate (data not shown), demonstrating that the Complex IV and the phosphorylation system are insensitive to alachlor in both models. Therefore, alachlor-induced ΔΨ dissipation and phosphorylation rate depression in glutamate/malate or succinate-energized mitochondria should be explained by the inhibitory action of the herbicide in the respiratory chain at the level of Complexes I and II, although an inhibition of Complex III cannot be excluded. This assumption is supported by the parallel inhibition of state 3- and FCCP uncoupled-respiration exerted by the herbicide, when malate/glutamate or succinate were used as respiratory substrates. The low stimulatory effect observed on state 4-respiration, suggested low ability of the compound to induce inner membrane permeabilization, excludes the involvement of proton leakage in alachlor-induced ΔΨ dissipation and phosphorylation rate depression. Interestingly, metolachlor, in a concentration range similar to that used here for alachlor, was also able to inhibit Complex I- and Complex II-, but not Complex IV-dependent respiration, and to promote a reduced effect on inner mitochondrial membrane permeability to protons (Pereira et al., 2009).

Considering the adverse effects of the two chloroacetanilide herbicides on rat liver mitochondria bioenergetics, it is reasonable to assume that mitochondria may have an important role in the toxicity caused by those compounds in non-target organisms. Concordant results had been previously described for the herbicide paraquat, which disturbed the respiratory electron transport chain and increased ROS levels in the mitochondrial matrix of *Caenorhabditis elegans* nematode (Edwards et al., 2013). Considering that mitochondria are the major source of ROS (Zorov et al., 2014), the increase in ROS levels observed in some organisms after alachlor treatment could result from direct effects in mitochondrial function, including inhibition of respiratory electron transport chain and/or mitochondrial ΔΨ dissipation (Burman et al., 2003; Gil et al., 2017) as observed in our study and simultaneously promoting the oxidative damage of several biological macromolecules.

Moreover, alachlor, as well as metolachlor (Pereira et al., 2009), exerted an inhibitory effect on oxygen consumption stimulated by NADH in *B. stearothermophilus* protoplasts, further emphasizing the importance of cellular respiration as a putative target for these chloroacetanilides and impact in bacteria, pointing to the ability to damage or change the community structure of the bacterial mats in the soil (Pereira et al., 2009).

The importance of lipids in the activity of respiratory complexes is well recognized (Serricchio et al., 2018; Anand et al., 2020). Indeed, membrane lipids, particularly cardiolipin, are required for both the stabilization of the complexes and the formation of supercomplexes (Serricchio et al., 2018; Anand et al., 2020). Although a direct interaction between the chloroacetanilide herbicides and the respiratory complexes should not be excluded, a disturbance of the physical properties of lipid environment, similar to that observed in DPPC liposomes, as detected by DSC and fluorescence polarization of DPH, might impact respiratory activity. Such perturbations, reflected in an increase of membrane fluidity and the induction of lateral phase separation with eventual repercussion on lipid-protein interactions and protein distribution in the plane of the membrane, could also contribute to the herbicide-induced inhibition of the growth of *B. stearothermophilus*. In this regard, it should be stressed that previous studies have shown that *B. stearothermophilus* growth is strictly dependent on the physical state of membrane lipids (Martins et al., 2003, 2005; Pereira et al., 2009).

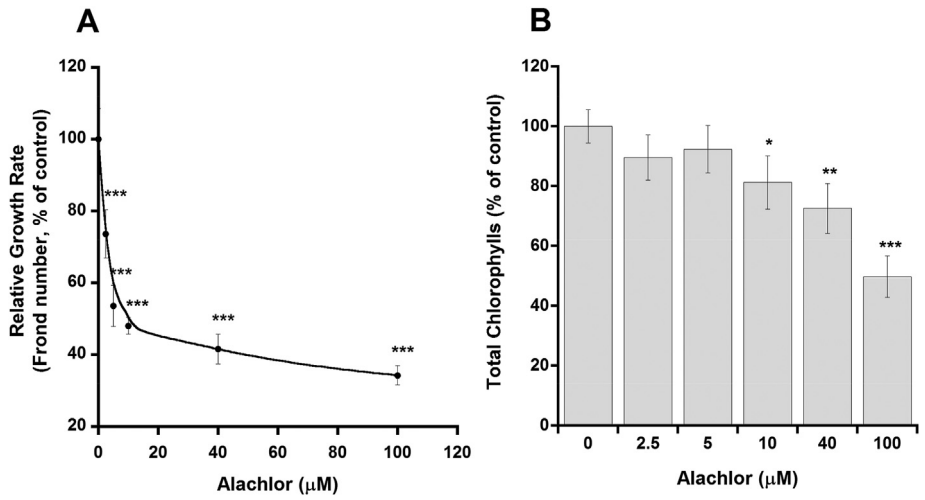

Fig. 6. Relative growth rate (**A**) and total chlorophylls (B) of *Lemna gibba* exposed for 7 days to increasing concentrations of alachlor. The relative growth rate (RGR) was calculated as described in Materials and Methods. Data are expressed as percentage of control (*Lemna gibba* in the absence of alachlor). All results represent the mean ± standard deviation of three independent experiments and comparasions relative to the control were performed using one-way ANOVA with the Student-Newman-Keuls as post hoc test (*$p < 0.05$; **$p < 0.01$; ***$p < 0.001$).

It is noteworthy that alachlor was more toxic to mammalian cells than to bacteria, promoting a depression of the bacterial growth rate to 50% at a concentration above 500 μM and reducing the viability of HeLa and neuro2a cells to 50% of the control at the concentrations of 235 and 69 μM, respectively. Taking into account that alachlor-induced toxicity is mediated by changes in membrane physical properties (Lushchak et al., 2018), as suggested by our DSC and fluorescence polarization data it is possible that, for example, neuronal cells which have plasma membranes with a peculiar lipid composition (enriched in glycolipids and higher lipid/protein ratio) (Lim and Wenk, 2009) can be more affected by alachlor-membrane interactions than HeLa cells. On the other hand, if mitochondria bioenergetics is involved in cell toxicity (Pereira et al., 2018; Deus et al., 2020), the higher severity of the effects exerted by alachlor on neuro2a cells as compared to HeLa cells could result from the higher susceptibility of brain mitochondria to toxicants. In fact, brain mitochondria, as compared to the same organelles of other tissues, namely liver, have been shown to be drastically affected by a large number of mitochondria-active compounds (Cunha-Oliveira et al., 2013; Moreira et al., 2013). An eventually higher partition of drugs into brain cell membranes and the lack of antioxidant enzymatic defenses (such as catalase) (Singhal et al., 2013) may be the reason for higher sensitivity of brain cells, and probably their organelles, to membrane-active compounds.

In the context of cell proliferation, evaluated in the three model systems, bacteria, mammalian cells and *Lemna gibba*, it is noteworthy that the latter was the most affected by alachlor. In terms of TC_{50}, a difference of about two orders of magnitude was observed between bacteria (>500 μM) or HeLa cells (235.5 μM) and *Lemna gibba* (7.8 μM). Most likely, alachlor caused a potent single effect on a vital metabolic function of *Lemna gibba* (Mohammad et al., 2010), which could explain the abrupt decrease of the plant growth rate at the lowest concentrations assayed. The disturbance of *Lemna gibba* proliferation was promoted by the herbicide at lower concentrations than those that induce the decay of chlorophylls. Therefore, we may conclude that, rather than chloroplast dysfunction, other processes, such as inhibition of protein synthesis and impairment of fatty acid metabolism (Yang et al., 2010; El-Nahhal and Hamdona, 2015), might have contributed to herbicide adverse effects on plant growth, at least at the lowest concentrations assayed. An impact on the distribution of the complexes of the photosynthetic system in chloroplast membranes or perturbations in lipid-protein interactions (Sharma et al., 2020), due to herbicide-induced changes in the physical behavior of membrane lipids showed by the biophysical studies, could also be evoked to explain herbicide adverse effects on *Lemna gibba.* In this context, the parallelism between the data provided by the different experimental models from prokaryotes to eukaryotes and from animal to plant systems, emphasizes the involvement of ubiquitous structures, such as membranes, as the primary target for the toxicity exerted by this chloroacetanilide herbicide (Santos et al., 2014; Nykiel-Szymańska et al., 2019; Kim et al., 2021). Thus, alachlor-induced perturbations of membrane physical properties might underlie a variety of effects leading to the disruption of the homeostasis in different biological systems, with predictable repercussion in their physiology (Kim et al., 2021). When a compound unspecific affects ubiquos structures such as lipidic membranes or mitochondria and the ability for energy production it is expected that it will affect several organisms (Santos et al., 2014). Starting toxicological assessment with these simple *in vitro* assays can save time and money on toxicological screening, reduce animal testing and harmful implications for the environment and humans.

In conclusion, the results obtained showed that alachlor-induced toxicity both in targeted and non-targeted organisms showed by TC_{50} values increased in the following order: *Lemna gibba* < neuro2a < HeLa cells < *Bacillus stearothermophilus*. Our work points out that the mechanism underlying the toxic action of this lipophilic herbicide is putatively mediated through interaction with biological membranes and perturbations of their physical properties, as well as the possible hazards of its dissemination on environment, compromising ecosystem equilibrium. Moreover, the parallelism between data obtained from the different experimental models emphasizes their suitability for chemical toxicity screening and stresses their usefulness to reduce the use of animals in toxicological assays and the pertinence of studying the differences in toxicity between difference species simultaneously exposed in order to prevent eco-toxicological risks and human health.

Authors' contributions

SPP, SMAS, MASF and JDM performed the experiments, the collection, the analysis and the interpretation of data, generated

figures and wrote the original draft. CMD make corrections to original draft of the manuscript. MCPL, JAFV, RAV and ASJ were responsible for funding acquisition and supervised the study. All authors revised the final form of the manuscript.

Declaration of competing interest

The authors declare that they have no known competing financial interests or personal relationships that could have appeared to influence the work reported in this paper.

Acknowledgements

This work was supported by the Portuguese Foundation for Science and Technology and FEDER/COMPETE and strategic project POCI-01-0145-FEDER-007440. SPP, JDM and CMD are recipients of fellowships from the Portuguese Foundation for Science and Technology (SFRH/BPD/116061/2016, SFRH/BD/73065/2010, SFRH/BD/100341/2014 respectively). The authors acknowledge the contribution from the Marine and Environmental Research Centre (IMAR-CMA) of the University of Coimbra, Portugal allowing access to equipment. The authors are extremely grateful to Karen Moore (University of Wyoming, USA) for English proofreading.

References

Acquavella, J.F., Delzell, E., Cheng, H., Lynch, C.F., Johnson, G., 2004. Mortality and cancer incidence among alachlor manufacturing workers 1968-99. Occup. Environ. Med. 61, 680–685.
Amer, S.M., Aly, F.A.E., Ibrahim, A.A.E., Farghaly, A.A., 2007. Cytogenetic effect of the chloroacetanilide herbicide alachlor in somatic and germ cells of the mouse. Cytologia 72, 7–15.
Anand, R., Kondadi, A.K., Meisterknecht, J., Golombek, M., Nortmann, O., Riedel, J., Peifer-Weiß, L., Brocke-Ahmadinejad, N., Schlütermann, D., Stork, B., Eichmann, T.O., Wittig, I., Reichert, A.S., 2020. MIC26 and MIC27 cooperate to regulate cardiolipin levels and the landscape of OXPHOS complexes. Life Sci. Alliance 3.
Badriyha, B.N., Ravindran, V., Den, W., Pirbazari, M., 2003. Bioadsorber efficiency, design, and performance forecasting for alachlor removal. Water Res. 37, 4051–4072.
Barbash, J.E., Thelin, G.P., Kolpin, D.W., Gilliom, R.J., 2001. Major herbicides in ground water: results from the National Water-Quality Assessment. J. Environ. Qual. 30, 831–845.
Bartlett, G.R., 1959 Mar. Phosphorus assay in column chromatography. J. Biol. Chem. 234 (3), 466–468 (PMID: 13641241).
Böger, P., 2003. Mode of action for chloroacetamides and functionally related compounds. J. Pestic. Sci. 28, 324–329.
Bora, S., Vardhan, G.S.H., Deka, N., Khataniar, L., Gogoi, D., Baruah, A., 2021. Paraquat exposure over generation affects lifespan and reproduction through mitochondrial disruption in C. elegans. Toxicology 447, 152632.
Böttcher, C.J.F., Van gent, C.M., Pries, C., 1961. A rapid and sensitive sub-micro phosphorus determination. Anal. Chim. Acta 24, 203–204.
Burman, D.M., Shertzer, H.G., Senft, A.P., Dalton, T.P., Genter, M.B., 2003. Antioxidant perturbations in the olfactory mucosa of alachlor-treated rats. Biochem. Pharmacol. 66, 1707–1715.
Cardoso, A.M.S., Faneca, H., Almeida, J.A.S., Pais, A.A.C.C., Marques, E.F., de Lima, M.C.P., Jurado, A.S., 2011. Gemini surfactant dimethylene-1,2-bis(tetradecyldimethylammonium bromide)-based gene vectors: a biophysical approach to transfection efficiency. Biochim. Biophys. Acta 1808, 341–351.
Chance, B., Williams, G.R., 1956. The respiratory chain and oxidative phosphorylation. Adv. Enzymol. Relat. Area Mol. Biol. 17, 65–134.
Chowdhary, P., Sammi, S.R., Pandey, R., Kaithwas, G., Raj, A., Singh, J., Bharagava, R.N., 2020. Bacterial degradation of distillery wastewater pollutants and their metabolites characterization and its toxicity evaluation by using Caenorhabditis elegans as terrestrial test models. Chemosphere 261, 127689.
Cunha-Oliveira, T., Silva, L., Silva, A.M., Moreno, A.J., Oliveira, C.R., Santos, M.S., 2013. Mitochondrial complex I dysfunction induced by cocaine and cocaine plus morphine in brain and liver mitochondria. Toxicol. Lett. 219, 298–306.
Deus, C.M., Pereira, S.P., Cunha-Oliveira, T., Pereira, F.B., Raimundo, N., Oliveira, P.J., 2020. Mitochondrial remodeling in human skin fibroblasts from sporadic male Parkinson's disease patients uncovers metabolic and mitochondrial bioenergetic defects. Biochim. Biophys. Acta (BBA) - Mol. Basis Dis. 1866, 165615.
Dludla, P.V., Jack, B., Viraragavan, A., Pheiffer, C., Johnson, R., Louw, J., Muller, C.J.F., 2018. A dose-dependent effect of dimethyl sulfoxide on lipid content, cell viability and oxidative stress in 3T3-L1 adipocytes. Toxicol Rep 5, 1014–1020.
Dovidauskas, S., Okada, I.A., Dos Santos, F.R., 2020. Validation of a simple ion chromatography method for simultaneous determination of glyphosate, aminomethylphosphonic acid and ions of Public Health concern in water intended for human consumption. J. Chromatogr. A 1632, 461603.
Eckermann, C., 2003. Covalent binding of chloroacetamide herbicides to the active site cysteine of plant type III polyketide synthases. Phytochemistry 64, 1045–1054.
Edwards, C.B., Copes, N., Brito, A.G., Canfield, J., Bradshaw, P.C., 2013. Malate and fumarate extend lifespan in Caenorhabditis elegans. PloS One 8, e58345.
El-Hadary, M.H., Chung, G., 2013. Herbicides — A Double Edged Sword, Herbicides - Current Research and Case Studies in Use. In: Kelton, A.J.P.a.J.A (Ed.). IntechOpen.
El-Nahhal, Y., Hamdona, N., 2015. Phytotoxicity of Alachlor, Bromacil and Diuron as single or mixed herbicides applied to wheat, melon, and molokhia. SpringerPlus 4, 367.
Fernandes, M.A.S., Pereira, S.P.S., Jurado, A.S., Custódio, J.B.A., Santos, M.S., Moreno, A.J.M., Duburs, G., Vicente, J.A.F., 2008. Comparative effects of three 1,4-dihydropyridine derivatives [OSI-1210, OSI-1211 (etaftoron), and OSI-3802] on rat liver mitochondrial bioenergetics and on the physical properties of membrane lipid bilayers: relevance to the length of the alkoxyl chain in. Chem. Biol. Interact. 173, 195–204.
Fernández, M., Ríos, J.C., Jos, A., Repetto, G., 2006. Comparative cytotoxicity of alachlor on RTG-2 trout and SH-SY5Y human cells. Arch. Environ. Contam. Toxicol. 51, 515–520.
Gil, F.N., Belli, G., Viegas, C.A., 2017. The Saccharomyces cerevisiae response to stress caused by the herbicidal active substance alachlor requires the iron regulon transcription factor Aft1p. Environ. Microbiol. 19, 485–499.
Gornall, A.G., Bardawill, C.J., David, M.M., 1949. Determination of serum proteins by means of the biuret reaction. J. Biol. Chem. 177, 751–766.
Grizard, G., Ouchchane, L., Roddier, H., Artonne, C., Sion, B., Vasson, M.P., Janny, L., 2007. In vitro alachlor effects on reactive oxygen species generation, motility patterns and apoptosis markers in human spermatozoa. Reprod. Toxicol. 23, 55–62.
Harper, A.P., Finger, B.J., Green, M.P., 2020. Chronic atrazine exposure beginning prenatally impacts liver function and sperm concentration with multigenerational consequences in mice. Front. Endocrinol. 11, 580124.
Hemanth Kumar, N.K., Jagannath, S., 2020. Cytological effects of herbicide alachlor in somatic cells of maize (Zea mays L.) and soybean (Glycine max Merrill.). Biocatal. Agric. Biotechnol. 24, 101560.
Jurado, A.S., Fernandes, M.A.S., Videira, R.A., Peixoto, F.P., Vicente, J.A.F., 2011. Herbicides : the face and the reverse of the coin. An in vitro Appr. Tox. Herb. Non-Target Org. 3–44.
Kean, E.F., Shore, R.F., Scholey, G., Strachan, R., Chadwick, E.A., 2021. Persistent pollutants exceed toxic thresholds in a freshwater top predator decades after legislative control. Environ. Pollut. 272, 116415.
Kim, H., Wang, H., Ki, J.S., 2021. Chloroacetanilides inhibit photosynthesis and disrupt the thylakoid membranes of the dinoflagellate Prorocentrum minimum as revealed with metazachlor treatment. Ecotoxicol. Environ. Saf. 211, 111928.
Koynova, R., Boyanov, A., Tenchov, B., 1985. On the phase diagram of an L-dipalmitoylphosphatidylcholine/cholesterol mixture. FEBS (Fed. Eur. Biochem. Soc.) Lett. 187, 65–68.
Kufel, L., Wysoki, U., Okni, S., Ry, K., 2012. Growth rate of duckweeds (Lemnaceae) in relation to the internal and ambient nutrient concentrations – testing the droop and monod models. Pol. J. Ecol. 60, 241–249.
Ladeira, C., Smajdova, L., 2017. The use of genotoxicity biomarkers in molecular epidemiology: applications in environmental, occupational and dietary studies. AIMS Genet 4, 166–191.
Lee, W.J., 2004. Cancer incidence among pesticide applicators exposed to alachlor in the agricultural health study. Am. J. Epidemiol. 159, 373–380.
Lerro, C.C., Andreotti, G., Koutros, S., Lee, W.J., Hofmann, J.N., Sandler, D.P., Parks, C.G., Blair, A., Lubin, J.H., Beane Freeman, L.E., 2018. Alachlor Use and Cancer Incidence in the Agricultural Health Study: an Updated Analysis. Journal of the National Cancer Institute.
Lichtenthaler, H.K., Wellburn, A.R., 1983. Determinations of total carotenoids and chlorophylls a and b of leaf extracts in different solvents. Biochem. Soc. Trans. 11, 591–592.
Lim, L., Wenk, M.R., 2009. Neuronal membrane lipids – their role in the synaptic vesicle cycle. In: Lajtha, A., Tettamanti, G., Goracci, G. (Eds.), Handbook of Neurochemistry and Molecular Neurobiology: Neural Lipids. Springer US, Boston, MA, pp. 223–238.
Lim, S., Ahn, S.Y., Song, I.C., Chung, M.H., Jang, H.C., Park, K.S., Lee, K.-U., Pak, Y.K., Lee, H.K., 2009. Chronic exposure to the herbicide, atrazine, causes mitochondrial dysfunction and insulin resistance. PloS One 4 e5186-e5186.
Lin, M.F., Wu, C.L., Wang, T.C., 1987. Pesticide clastogenicity in Chinese hamster ovary cells. Mutat. Res. 188, 241–250.
Lushchak, V.I., Matviishyn, T.M., Husak, V.V., Storey, J.M., Storey, K.B., 2018. Pesticide toxicity: a mechanistic approach. EXCLI J 17, 1101–1136.
Machado, N.G., Baldeiras, I., Pereira, G.C., Pereira, S.P., Oliveira, P.J., 2010. Subchronic administration of doxorubicin to Wistar rats results in oxidative stress and unaltered apoptotic signaling in the lung. Chem. Biol. Interact. 188, 478–486.
Marc, J., Mulner-Lorillon, O., Boulben, S., Hureau, D., Durand, G., Bellé, R., 2002. Pesticide Roundup provokes cell division dysfunction at the level of CDK1/cyclin B activation. Chem. Res. Toxicol. 15, 326–331.
Martins, J.D., Jurado, A.S., Moreno, A.J.M., Madeira, V.M.C., 2005. Comparative study of tributyltin toxicity on two bacteria of the genus Bacillus. Toxicol. Vitro 19, 943–949.

Martins, J.D., Monteiro, J.P., Antunes-Madeira, M.C., Jurado, A.S., Madeira, V.M.C., 2003. Use of the microorganism Bacillus stearothermophilus as a model to evaluate toxicity of the lipophilic environmental pollutant endosulfan. Toxicol. Vitro 17, 595–601.
Maxfield, F.R., Tabas, I., 2005. Role of cholesterol and lipid organization in disease. Nature 438, 612–621.
Mhadhbi, L., Beiras, R., 2016. Retraction note: acute toxicity of seven selected pesticides (alachlor, atrazine, dieldrin, diuron, pirimiphos-methyl, chlorpyrifos, diazinon) to the marine fish (turbot, psetta maxima). Water, Air, Soil Pollut. 227, 275.
Mnif, W., Hassine, A.I.H., Bouaziz, A., Bartegi, A., Thomas, O., Roig, B., 2011. Effect of endocrine disruptor pesticides: a review. Int. J. Environ. Res. Publ. Health 8, 2265–2303.
Mohammad, M., Itoh, K., Suyama, K., 2010. Effects of herbicides on Lemna gibba and recovery from damage after prolonged exposure. Arch. Environ. Contam. Toxicol. 58, 605–612.
Moreira, A.C., Silva, A.M., Santos, M.S., Sardão, V.A., 2013. Resveratrol affects differently rat liver and brain mitochondrial bioenergetics and oxidative stress in vitro: investigation of the role of gender. Food Chem. Toxicol. : Int. J. Publ. Brit. Indus. Biol. Res. Assoc. 53, 18–26.
Nykiel-Szymańska, J., Różalska, S., Bernat, P., Słaba, M., 2019. Assessment of oxidative stress and phospholipids alterations in chloroacetanilides-degrading Trichoderma spp. Ecotoxicol. Environ. Saf. 184, 109629.
OECD, 2002. Guidelines for the Testing of Chemicals. Environment Directorate, Organisation for Economic Cooperation and Development.
Osano, O., Admiraal, W., Otieno, D., 2002. Developmental disorders in embryos of the frog Xenopus laevis induced by chloroacetanilide herbicides and their degradation products. Environ. Toxicol. Chem./SETAC 21, 375–379.
Park, H., Lee, J.Y., Lim, W., Song, G., 2021. Assessment of the in vivo genotoxicity of pendimethalin via mitochondrial bioenergetics and transcriptional profiles during embryogenesis in zebrafish: implication of electron transport chain activity and developmental defects. J. Hazard Mater. 411, 125153.
Pereira, S.P., Deus, C.M., Serafim, T.L., Cunha-Oliveira, T., Oliveira, P.J., 2018. Metabolic and phenotypic characterization of human skin fibroblasts after forcing oxidative capacity. Toxicol. Sci. 164, 191–204.
Pereira, S.P., Fernandes, M.A.S., Martins, J.D., Santos, M.S., Moreno, A.J.M., Vicente, J.a.F., Videira, R.A., Jurado, A.S., 2009. Toxicity assessment of the herbicide metolachlor comparative effects on bacterial and mitochondrial model systems. Toxicol. Vitro 23, 1585–1590.
Perreault, F., Oukarroum, A., Pirastru, L., Sirois, L., Gerson Matias, W., Popovic, R., 2010. Evaluation of copper oxide nanoparticles toxicity using chlorophyll a fluorescence imaging in Lemna gibba. J. Bot/ 1–9, 2010.
Piel, S., Grandcoin, A., Baurès, E., 2021. Understanding the origins of herbicides metabolites in an agricultural watershed through their spatial and seasonal variations. J Environ Sci Health B 1–17.
Rattanawong, K., Kerdsomboon, K., Auesukaree, C., 2015. Cu/Zn-superoxide dismutase and glutathione are involved in response to oxidative stress induced by protein denaturing effect of alachlor in Saccharomyces cerevisiae. Free Radical Biol. Med. 89, 963–971.
Ryberg, K.R., Gilliom, R.J., 2015. Trends in pesticide concentrations and use for major rivers of the United States. Sci. Total Environ. 538, 431–444.
Sadura, I., Latowski, D., Oklestkova, J., Gruszka, D., Chyc, M., Janeczko, A., 2020. Molecular dynamics of chloroplast membranes isolated from wild-type barley and a brassinosteroid-deficient mutant acclimated to low and high temperatures. Biomolecules 11.
Santos, S.M.a., Dinis, A.M., Rodrigues, D.M.F., Peixoto, F., Videira, R.a., Jurado, A.S., 2013. Studies on the toxicity of an aqueous suspension of C60 nanoparticles using a bacterium (gen. Bacillus) and an aquatic plant (Lemna gibba) as in vitro model systems. Aquat. Toxicol. 142–143, 347–354.
Santos, S.M.a., Videira, R.a., Fernandes, M.a.S., Santos, M.S., Moreno, A.J.M., Vicente, J.a.F., Jurado, A.S., 2014. Toxicity of the herbicide linuron as assessed by bacterial and mitochondrial model systems. Toxicol. Vitro 28, 932–939.
Seok, S.-J., Choi, S.-C., Gil, H.-W., Yang, J.-O., Lee, E.-Y., Song, H.-Y., Hong, S.-Y., 2012. Acute oral poisoning due to chloracetanilide herbicides. J. Kor. Med. Sci. 27, 111–114.
Serricchio, M., Vissa, A., Kim, P.K., Yip, C.M., McQuibban, G.A., 2018. Cardiolipin synthesizing enzymes form a complex that interacts with cardiolipin-dependent membrane organizing proteins. Biochim. Biophys. Acta Mol. Cell Biol. Lipids 1863, 447–457.
Sharma, A., Kumar, V., Shahzad, B., Ramakrishnan, M., Singh Sidhu, G.P., Bali, A.S., Handa, N., Kapoor, D., Yadav, P., Khanna, K., Bakshi, P., Rehman, A., Kohli, S.K., Khan, E.A., Parihar, R.D., Yuan, H., Thukral, A.K., Bhardwaj, R., Zheng, B., 2020. Photosynthetic response of plants under different abiotic stresses: a review. J. Plant Growth Regul. 39, 509–531.
Shinitzky, M., Barenholz, Y., 1978. Fluidity parameters of lipid regions determined by fluorescence polarization. Biochim. Biophys. Acta 515, 367–394.
Silva, F.S., Starostina, I.G., Ivanova, V.V., Rizvanov, A.A., Oliveira, P.J., Pereira, S.P., 2016. Determination of metabolic viability and cell mass using a tandem resazurin/sulforhodamine B assay. Curr. Protocol Toxicol. 68, 2 24 21-22 24 15.
Singhal, A., Morris, V.B., Labhasetwar, V., Ghorpade, A., 2013. Nanoparticle-mediated catalase delivery protects human neurons from oxidative stress. Cell Death Dis. 4 e903-e903.
Sopeña, F., Maqueda, C., Morillo, E., 2009. Formulation affecting alachlor efficacy and persistence in sandy soils. Pest Manag. Sci. 65, 761–768.
Tekpli, X., Holme, J.A., Sergent, O., Lagadic-Gossmann, D., 2013. Role for membrane remodeling in cell death: implication for health and disease. Toxicology 304, 141–157.
Trenkamp, S., Martin, W., Tietjen, K., 2004. Specific and differential inhibition of very-long-chain fatty acid elongases from Arabidopsis thaliana by different herbicides. Proc. Natl. Acad. Sci. U.S.A. 101, 11903–11908.
WHO, 2017. Guidelines for Drinking-Water Quality: Fourth Edition Incorporating the First Addendum. © World Health Organization 2017., Geneva.
Wisdom, C., Welker, N.E., 1973. Membranes of Bacillus stearothermophilus: factors affecting protoplast stability and thermostability of alkaline phosphatase and reduced nicotinamide adenine dinucleotide oxidase. J. Bacteriol. 114, 1336–1345.
Yang, X., Guschina, I.A., Hurst, S., Wood, S., Langford, M., Hawkes, T., Harwood, J.L., 2010. The action of herbicides on fatty acid biosynthesis and elongation in barley and cucumber. Pest Manag. Sci. 66, 794–800.
Yi, X., Ding, H., Lu, Y., Liu, H., Zhang, M., Jiang, W., 2007. Effects of long-term alachlor exposure on hepatic antioxidant defense and detoxifying enzyme activities in crucian carp (Carassius auratus). Chemosphere 68, 1576–1581.
Yuan, Y., Liu, X., Liu, T., Liu, W., Zhu, Y., Zhang, H., Zhao, C., 2020. Molecular dynamics exploring of atmosphere components interacting with lung surfactant phospholipid bilayers. Sci. Total Environ. 743, 140547.
Zamprogno, P., Wüthrich, S., Achenbach, S., Thoma, G., Stucki, J.D., Hobi, N., Schneider-Daum, N., Lehr, C.M., Huwer, H., Geiser, T., Schmid, R.A., Guenat, O.T., 2021. Second-generation lung-on-a-chip with an array of stretchable alveoli made with a biological membrane. Comm. Biol. 4, 168.
Zhang, C., Qin, L., Dou, D.C., Li, X.N., Ge, J., Li, J.L., 2018. Atrazine induced oxidative stress and mitochondrial dysfunction in quail (Coturnix C. coturnix) kidney via modulating Nrf2 signaling pathway. Chemosphere 212, 974–982.
Zorov, D.B., Juhaszova, M., Sollott, S.J., 2014. Mitochondrial reactive oxygen species (ROS) and ROS-induced ROS release. Physiol. Rev. 94, 909–950.